Journal of Electroceramics, 13, 35–39, 2004

Influence of the Lead Source Materials on the Microstructure and Ferroelectric Properties of PZT Films Sputter-Deposited Using Lead and Lead Oxide

W.L. CHANG* & J.L. HE

Department of Materials Science, Feng Chia University, Taichung, Taiwan

Submitted February 13, 2003; Revised January 30, 2004; Accepted February 2, 2004

Abstract. In this investigation, PZT films were sputter-deposited on $Si/SiO_2/Ti/Pt$ substrates using a dual-target system. The dual targets $Pb/PZT(PbZr_{0.54}Ti_{0.46}O_3)$ and $PbO/PZT(PbZr_{0.54}Ti_{0.46}O_3)$ were used to reveal the effects of various lead compensation source materials on the microstructure and ferroelectric properties of the films. The structures of the films were characterized by X-ray diffractometry (XRD) and field emission scanning electron microscopy (FESEM). The chemical binding state was determined using X-ray photoelectron spectrometry (XPS). Ferroelectric polarizability was measured using a Radiant Technology RT66A tester. The influence of deposition temperatures on the microstructure and ferroelectric properties of the films was studied. Perovskite PZT films were successfully deposited using the Pb/PZT and the PbO/PZT dual target sputtering systems at a substrate temperature of between 500 and 580°C. Structural change was elucidated as a function of deposition temperatures and the lead sources were correlated with the ferroelectric properties of the film. The ferroelectric characteristics of the PZT films deposited using the PbO/PZT dual target were better than those of films deposited using the Pb/PZT dual target, because the former films had a higher bonding energy.

Keywords: PZT film, Pb compensation, microstructure, ferroelectric properties

Introduction

Ferroelectric materials such as lead-zirconate-titanate ($Pb(Zr_x,Ti_{1-x})O_3$,PZT) films exhibit ferroelectricity, piezoelectricity, electro-optical characteristics and spontaneous polarization. These properties enable PZT films to be used in a broad range of device applications, such as surface acoustic wave (SAW) devices, sensors, non-volatile random-access memories (NVRAMs), accelerometers and transducers, among others [1, 2].

PZT films have been prepared by various deposition techniques, including metal organic chemical vapor deposition (MOCVD) [3–5], sol-gel processing [6–12], laser ablation [13–17] reactive evaporation [18] and sputtering [19–23]. The preparation of PZT films by sputter deposition techniques, using various source materials, has attracted much interest recently [22, 24]. The PbO/PZT dual target system has become well established as enabling the lead flux to be controlled precisely to compensate for the lead deficiency during PZT deposition. Preparing the PbO target material is difficult because a high vapor pressure is required during sintering. Substitution with metallic Pb facilitates the fabrication of the target material and enables dc sputtering. Such a Pb/PZT combination has been rarely studied.

In this investigation, PZT thin films were deposited on $Pt/Ti/SiO_2/Si$ substrate using both Pb/PZT and PbO/PZT dual target systems, to reveal the effect of the source materials used to compensate for the lead deficiency on the microstructure and ferroelectric properties of the films. Microstructural changes and ferroelectric properties were considered in relation to the deposition temperatures.

*To whom all correspondence should be addressed. E-mail: cwl@tbnet.org.tw

Table 1. Deposition conditions of the PZT films.

Target combination	Pb/PZT dual target	PbO/PZT dual target
RF power (W)	PZT:80, Pb:25	PZT:80, PbO:30
Target diameter	75 mm	
Sputtering gas	Ar	
Working pressure	0.15 Pa	
Deposition time	2 h	
Substrate temperature	Ambient temperature to 580°C	
Substrate material	Pt/Ti/SiO_2/Si	

Experimental

Table 1 presents the deposition conditions of the PZT films. The two dual target combinations were Pb/PZT($PbZr_{0.54}Ti_{0.46}O_3$) and PbO/PZT($PbZr_{0.54}Ti_{0.46}O_3$). The RF powers of Pb/PZT and PbO/PZT were kept constant at 25W/80W and 30W/80W, respectively. The substrate temperatures were varied from ambient temperature to 580°C. Pt(150 nm)/Ti(50 nm)/SiO_2(150 nm)/Si was used as a substrate material.

The crystal structures of the deposited PZT films were determined using XRD. The cross-sectional morphology of the deposited PZT films was observed using FESEM. XPS, in combination with a sputter etching gun, was used to reveal the chemical state of the Pb element throughout the thickness of the film. Ferroelecrtric polarization was measured using Radiant Technology's RT66A tester.

Results and Discussions

Figure 1 presents the cross-sectional morphology and the growth rate of the PZT film deposited using Pb/PZT and PbO/PZT dual targets at various substrate temperatures. At the ambient temperature, the PZT films appeared to have smooth surface and featureless cross-sections, as shown in Figs. 1(a) and (b). In contrast, the films deposited at a higher substrate temperature of 580°C, as indicated in Figs. 1(c) and (d) exhibit columnar grain growth from the bottom electrode layer of Pt, representing an increase in thickness due to Pt/PZT or Pt/Si substrate interdiffusion.

One difference between using the Pb/PZT and the PbO/PZT dual target combinations is the resulting thickness of the film. Figure 1 shows growth rate versus substrate temperature. Although the target power

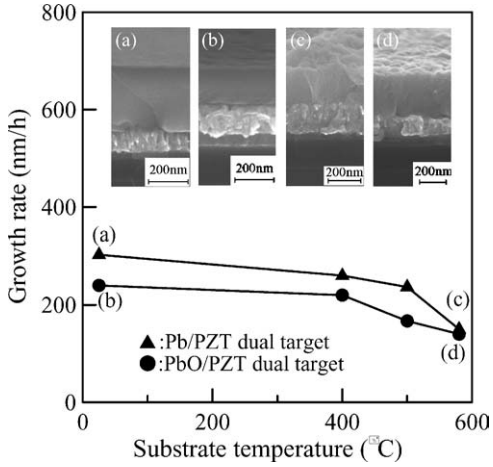

Fig. 1. Cross-sectional morphology and growth rate of the PZT films as a function of substrate temperatures, obtained using Pb/PZT and PbO/PZT dual target systems. Deposition time was 2 hr.

of the Pb target is less than that of the PbO target, the growth rate of the films deposited using the Pb/PZT dual target exceeds that of the films deposited using the PbO/PZT dual target because the sputter yield of Pb exceeds that of PbO. The growth rate also declined as the substrate temperature increased for both dual target combinations, which result is considered to be a result of competition driven by the difference between the activation energy of the lower-temperature phases and that of the higher-temperature phases. Furthermore, the high evaporation pressure of Pb also reduces the thickness of the film. For both dual target systems, the phases formed in the deposited films changed as the substrate temperature increased, as shown in Fig. 2.

The PZT films deposited at ambient temperature using Pb/PZT dual target were found to be amorphous structures and the perovskite phase and α-PbO_2 phase coexisted at 500°C. The films become predominantly perovskite phase at 580°C. The coexistence of pryochlore and Pb_3O_4 phases is observed in the PZT films deposited using PbO/PZT dual target system at 400°C. The films become predominantly perovskite phase over 500°C, as shown in Fig. 2(b). The results demonstrate that lower substrate temperatures can be attained when a PbO/PZT dual target combination is used rather than using a Pb/PZT dual target system. Optimization of PbO target power also allows the perovskite phase to be formed at lower substrate temperatures. Moreover, less perovskite phase is deposited at 500°C than can

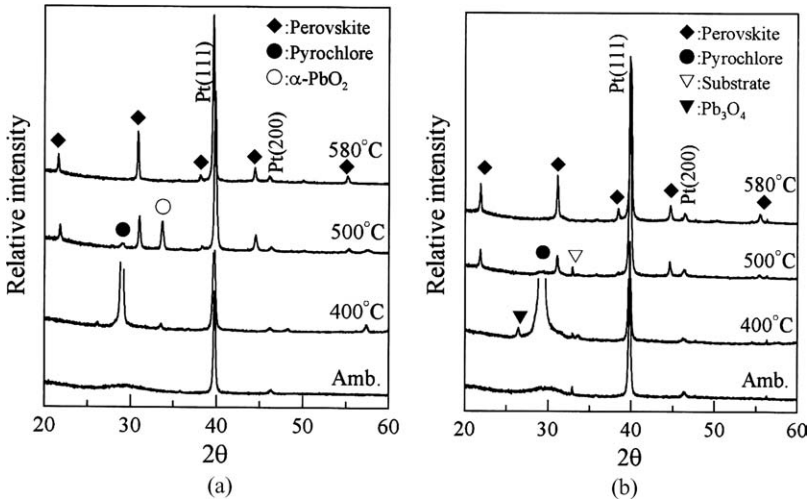

Fig. 2. XRD patterns of PZT films at various substrate temperatures, obtained using: (a) Pb/PZT and (b) PbO/PZT dual target systems.

be deposited using other processing methods, such as sol-gel [25], MOCVD [26] and other sputtering processes [27, 28]. These results reveal that the perovskite phase can be deposited using a Pb/PZT dual target at 580°C. Nevertheless, the PbO/PZT dual target appears to favor the formation of the perovskite phase at a lower substrate temperature.

The high-resolution spectra of the Pb_{4f} photoelectron lines of the PZT films deposited using the dual target systems at 580°C are shown in Figs. 3(a) and (b) as a function of Ar^+ ion sputtering times, to understand more about the chemical binding state of the deposited films. Figure 3(a) reveals that the Pb_{4f} presents two peaks 137.4 and 142.4 eV at the top film surface, corresponding to Pb in PbO because the exposure of the film to the atmosphere after deposition leads to oxidation [4]. After a sputtering time of 500 seconds, the $Pb_{4f7/2}$ and $Pb_{4f5/2}$ peaks shift to a constant value of 136.6 and 141.5 eV, attributable to Pb in PZT [8]. The binding energies of Pb_{4f} at the top surface of the PZT film deposited using the PbO/PZT dual target are 137.2 and 141.9 eV; they shift to lower binding energies of

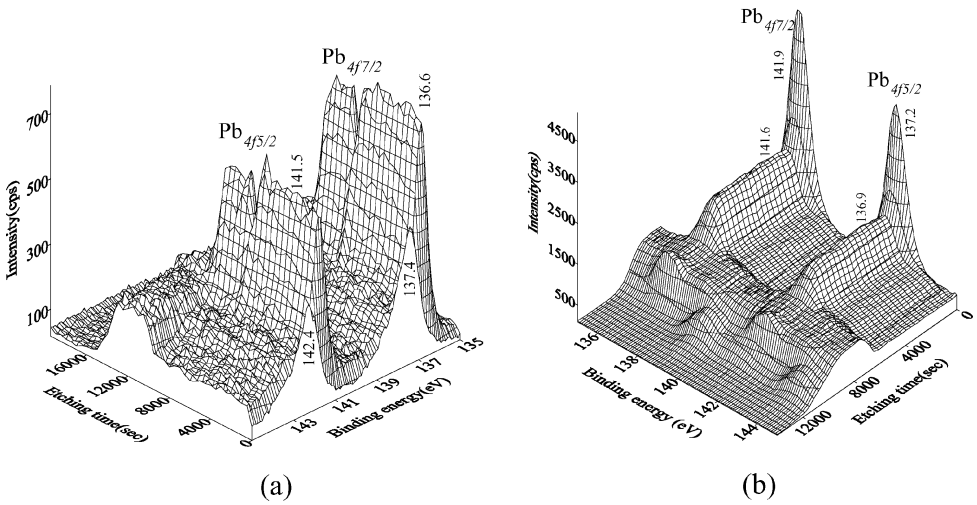

Fig. 3. Narrow scan spectra of Pb_{4f} of PZT films deposited using: (a) Pb/PZT and (b) PbO/PZT dual target systems at a substrate temperature of 580°C.

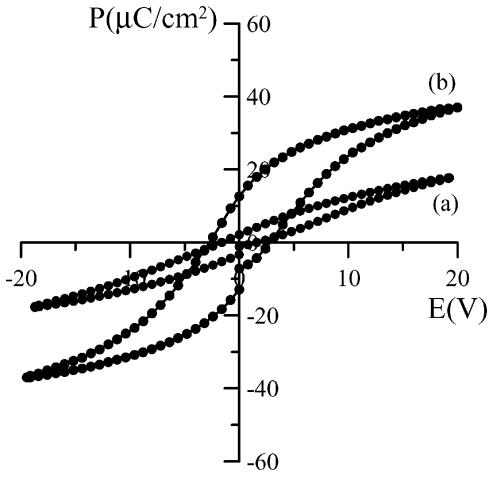

Fig. 4. Polarization behavior of PZT films deposited using: (a) Pb/PZT and (b) PbO/PZT dual target systems at a substrate temperature of 580°C.

136.9 and 141.6 eV as the etching time is increased, resembling the behavior of the film deposited by the Pb/PZT dual-target system. The PbO oxide layer on the top surface of the PZT films obtained using the sol-gel process [8] indicates the ease of PZT oxidization on the surface driven by the surface energy. The chemical states of the PZT films deposited by the two dual target combination do not significantly differ, according to XPS analysis.

Figure 4 shows that the PZT film deposited using the PbO/PZT dual target exhibits greater saturation polarization than that of the Pb/PZT dual target, with both obtained at a substrate temperature of 580°C. At a lower substrate temperature, both dual systems exhibit paraelectricity.

Conclusion

Perovskite PZT films can be deposited on a $Si/SiO_2/Ti/Pt$ substrate using either Pb/PZT or PbO/PZT dual target RF magnetron sputtering systems. The perovskite phase was formed at a high deposition temperature, but, at lower temperatures when a PbO/PZT dual target was used. The chemical states of Pb_{4f} in the PZT films deposited by these dual target combinations do not significantly differ; however, the film deposited using the PbO/PZT dual target had a higher saturation/remanent polarization than that of the film deposited using the Pb/PZT dual target.

Acknowledgment

The authors would like to thank the National Science Council of Taiwan, ROC, for financially supporting this research under Contract No. NSC90-2745-P-035-004 Prof. K.C. Chen of the Department of Materials Science, Feng Chia University, is appreciated for his valuable discussions. Miss H.P. Wen's help at the Instrumentation Center of National Taiwan University in conducting XPS analysis are also greatly appreciated.

References

1. M. Sayer and K. Sreenivas, *Science*, **247**, 1056 (1990).
2. T. Shiosak, *Ultrason. Symp. Proc.*, *IEEE*, 537(1990).
3. N. Wakiya, K. Kuroyanagi, Y. Xuan, K. Shinozaki, and N. Mizutani, *Thin Solid Films*, **372**, 156 (2000).
4. J.N. Kim, K.S. Shin, D.H. Kim, B.O. Park, N.K. Kim, and S.H. Cho, *Applied Surface Science*, **206**(1–4), 119 (2003).
5. M. Cerqueira, R.S. Nasar, E.R. Leite, E. Longo, and J.A. Varela, *Ceram. Int.*, **26**(3), 231 (2000).
6. M.G. Kang, K.T. Kim, and C.I. Kim, *Thin Solid Films*, **398–399**, 448 (2001).
7. O. Sugiyami, Y. Kondo, H. Suzuki, and S. Kaneko, *J. Sol-Gel Soc. Technol.*, **26**, 749 (2003).
8. C.R. Cho, *Cryst. Res. Technol.*, **35**(1), 77 (2000).
9. N. Ozer and T. Sands, *J. Sol-Gel Sci. Technol.*, **19**(1–3), 157 (2000).
10. C.R. Cho, L.F. Francis, and D.L. Polla, *Mater. Lett.*, **38**(2), 125 (1999).
11. S.A. Impey, Z. Huang, and A. Patel, *J. Appl. Phys.*, **83**(4), 2202 (1998).
12. R. Bruchhaus, *Ferroelectrics*, **133**(1–4), 73 (1992).
13. N.J. Wu, A. Ignatiev, A.W. Mesarwi, H. Lin, K. Xan, and H.D. Shih, *Mater. Chem. Phys.*, **32**, 5019 (1993).
14. A.R. Zomorrodian, A. Messarwi, N.J. Wu, and A. Ignatiev, *Appl. Surf. Sci.*, **90**, 343 (1995).
15. P. Verardi, F. Craciun, L. Mirenghi, M. Dinescu, and V. Sandu, *Appl. Surf. Sci.*, **138–139**, 552 (1999).
16. A.R. Zomorrodian, A.M.A., and N.J. Wu, *Ceram. Int.*, **25**(2), 137 (1999).
17. H. Kidoh, T. Ogawa, H. Yashima, A. Morimoto, and T. Shimizu, *Jpn. J. Appl. Phys. Pt.*1, **31**, 2965 (1992).
18. S. Takatani, H. Keiko, K.A. Keiko, and K. Torii, *J. Appl. Phys.*, **85**(11), 7784 (1999).
19. C.W. Chung, Y.H. Byun, and H.I. Kim, *Microelectron. Eng.*, **63**(4), 353 (2002).
20. W.Y. Choi and H.G. Kim, *Jpn. J. Appl. Phys.*, **138**(1A), 122 (1999).
21. W.Y. Choi, J.H. Ahn, and W.J. Lee, *Mater. Lett.*, **37**(3), 119 (1998).
22. K. Iijima, I. Ueda, and K. Kugimiya, *Jpn. J. Appl. Phys. Pt.*1, **30**(9B), 2149 (1991).

23. T. Hase and T. Shiosaki, *Jpn. J. Appl. Phys. Pt.*1, **30**(9B), 2159 (1991).
24. S. Yamauchi and M. Yoshimaru, *Jpn. J. Appl. Phys.*, **35**, 1553 (1996).
25. L.N. Chapin and S.A. Myers, *Mater. Res. Soc. Symp. Proc.*, **243**, 153 (1992).
26. M.D. Keijser and D.J.M. Dormans, *MRS Bull*, **21**, 37 (1996).
27. C.K. Kwok and S.B. Desu, *Ceram. Trans.*, **25**, 85 (1992).
28. T.S. Kim, D.J. Kim, J.K. Lee, and H.J. Jung, *J. Vac. Sci. Technol.*, **A15**(6), 2831 (1997).